Sensors and Actuators A 193 (2013) 238–245

Contents lists available at SciVerse ScienceDirect

Sensors and Actuators A: Physical

journal homepage: www.elsevier.com/locate/sna

Lubrication of polycrystalline silicon MEMS via a thin silicon carbide coating

Ian Laboriante[1], Anton Suwandi, Carlo Carraro, Roya Maboudian*

Department of Chemical and Biomolecular Engineering, University of California, Berkeley, CA 94720, USA

ARTICLE INFO

Article history:
Received 31 August 2011
Received in revised form
21 September 2012
Accepted 15 January 2013
Available online 24 January 2013

Keywords:
MEMS
High aspect ratio structures
Polycrystalline silicon
Silicon carbide
Solid lubrication
Stiction
Surface modification
Wear resistance

ABSTRACT

The contacting surfaces of a microfabricated polycrystalline silicon (polysilicon) double-clamped beam adhesion test structure have been modified with a thin ultra-hard, wear-resistant, and conformal silicon carbide (SiC) film. Adhesion forces in SiC-coated interfaces as a function of apparent area of contact have been determined quantitatively and compared with those in uncoated polysilicon contacts. Furthermore, contact reliability studies have been carried out by following the changes in physicochemical properties of the surfaces after >100 billion contact cycles. The results highlight the tribological benefits of SiC coating as a solid lubricant in devices undergoing cyclic contacts.

1. Introduction

Successful deployment of silicon-based microelectromechanical systems (MEMS) necessitates proper passivation and lubrication of the contacting surfaces to prevent irreversible interfacial adhesion (*stiction*) and wear [1–4]. Unwanted adhesion, more commonly known as *stiction*, remains a common failure mechanism in silicon-based microelectromechanical systems and in advanced microelectronics with high aspect ratio structures due to a variety of factors, including propensity of silicon to form a layer of hydrophilic, high surface energy native oxide [2,5]. Although release-related *stiction* has been addressed through several schemes including vapor HF [6–9], critical point drying [10–13], by roughening the surfaces [14,15], or by self-assembled monolayer coating schemes [16–21], in-use *stiction* still poses a significant issue to the reliability of MEMS. This phenomenon occurs when surface forces such as van der Waals, capillary, and/or electrostatic force dominate over the restoring force and causes a malfunction during device operation. The rough contacting surfaces of microfabricated structures built out of polysilicon have been also shown to be mechanically weak due to high contact pressures generated at the asperity contacts. As a consequence, it is expected that silicon microstructures designed for repetitive contacts during operation likely fail due to wear which severely limits the lifetime of the devices. Additionally, silicon-based MEMS are challenged for operating under harsh environmental conditions of elevated temperatures, oxidative and corrosive environments, and in mechanically demanding applications, e.g., for combustion monitoring and power generation [22–25].

One effective way to resolve these reliability issues is by coating the wafers with a thin silicon carbide layer across the surface to reduce the surface energy of the device [26]. SiC is a material of choice for solid lubrication in polysilicon MEMS due to its many outstanding properties, including the ability to tailor its doping level to enhance conductivity and minimize charging, high specific strength and creep resistance, thermal stability and conductivity, chemical inertness, mechanical strength (hard), wear resistance, low surface energy, hydrophobic, and the synthesis ability for conformal coating of surfaces that are not in line of sight. The incorporation of ultra-hard, wear-resistant, and conformal SiC hard coatings in MEMS architecture takes advantage of these attractive properties and at the same time allows the preservation of the overall microsystem design.

With the introduction of a new tribological interface, that of the SiC coating that interacts directly with adsorbates or lubricant species present in the operating environment, it is desirable to study and predict the failure mechanisms sooner than they occur in normal MEMS operation to pave the way for full scale implementation of MEMS to the mainstream. Experimentally, adhesion forces in polycrystalline SiC (polySiC) interface as a function

* Corresponding author. Tel.: +1 510 643 7957.
E-mail addresses: maboudia@berkeley.edu, maboudia@socrates.berkeley.edu (R. Maboudian).
[1] Present address: Micron Technology, Boise, ID 83707, USA.

0924-4247/$ – see front matter © 2013 Elsevier B.V. All rights reserved.
http://dx.doi.org/10.1016/j.sna.2013.01.036

of apparent contact area have been determined quantitatively using a microfabricated test structure. This paper also presents a detailed, systematic study of the evolution of physicochemical properties of the interface for over 100 billion contact cycles. The correlated results of adhesion and lifetime studies are then compared to those obtained on polysilicon interfaces with comparable topography.

2. Experimental details

2.1. Device structure, fabrication and surface modification

An array of double-clamped beam (DCB) test structures designed to measure adhesion forces in micrometer-scale surface interactions were fabricated through standard PolyMUMPS (MEMSCAP, Inc.) multilayer micromachining processes. The fabrication processes including the release procedure are described in detail in Ref. [27]. Fig. 1(a)–(c) depicts the schematic top and side views of the fabricated DCB test structure illustrating both non-contact and contact states. The beam (also called source electrode by convention) is suspended 2 μm above a landing pad (drain electrode) and two symmetrically positioned actuation pads through which the actuation (bias) voltage is applied. A representative scanning electron microscopy (SEM) image of a DCB device with 275 μm long beam is shown in Fig. 1(d). The beam and the landing pad are both grounded. An extra probe pad attached to the drain electrode is designed to enable four-point current vs. voltage (I–V) measurements. A dimple with 0.75 μm thickness is incorporated in the middle of the beam and directly above landing pad to define the apparent area of contact. The separation between the dimple and the landing pad is 1.25 μm.

A series of DCB test structures with 275 and 350 μm long beams and with dimple sizes in the range from 4 μm × 4 μm to 12 μm × 12 μm were used for this study. The devices were released [27] and then coated with SiC film. The SiC layer was deposited on the released structures via low pressure chemical vapor deposition (LPCVD) using disilabutane (DSB) precursor. The LPCVD reactor (TekVac) was pumped down to a base pressure of $<5 \times 10^{-6}$ Torr. The gas phase DSB reagent was introduced at a flow rate of 5 sccm for 4 min at a reactor temperature of 780 °C. The resultant SiC layer has a thickness of 50 nm as determined by prior calibration done on a separate flat Si(1 0 0) substrate and verified through AFM measurements. The film also yielded a smoother surface with an average root-mean-square (rms) roughness of 10.2 nm in comparison with as-released polysilicon substrate which has an rms roughness of ~15.1 nm. After SiC layer deposition, the separation between the beam and a landing pad is decreased from 1.25 μm to 1.15 μm. A bias of ~75 V is typically required to actuate a 275 μm long SiC-coated DCB into contact with the landing pad, whereas polysilicon DCB of the same length requires ~25 V. The DCB design was chosen to ensure symmetric contact and enable precise measurements of adhesion forces using a methodology outlined in Refs. [27,28].

2.2. Measurement of adhesion forces

Adhesion measurements using DCB devices were carried out in a similar scheme to that reported previously [27,28]. For direct comparison, similar measurements were done on as-fabricated (native oxide-coated) polysilicon structures and on SiC-coated structures. Optical interferometric techniques have been used to systematically determine the beam profile and the pull-in and pull-off voltage

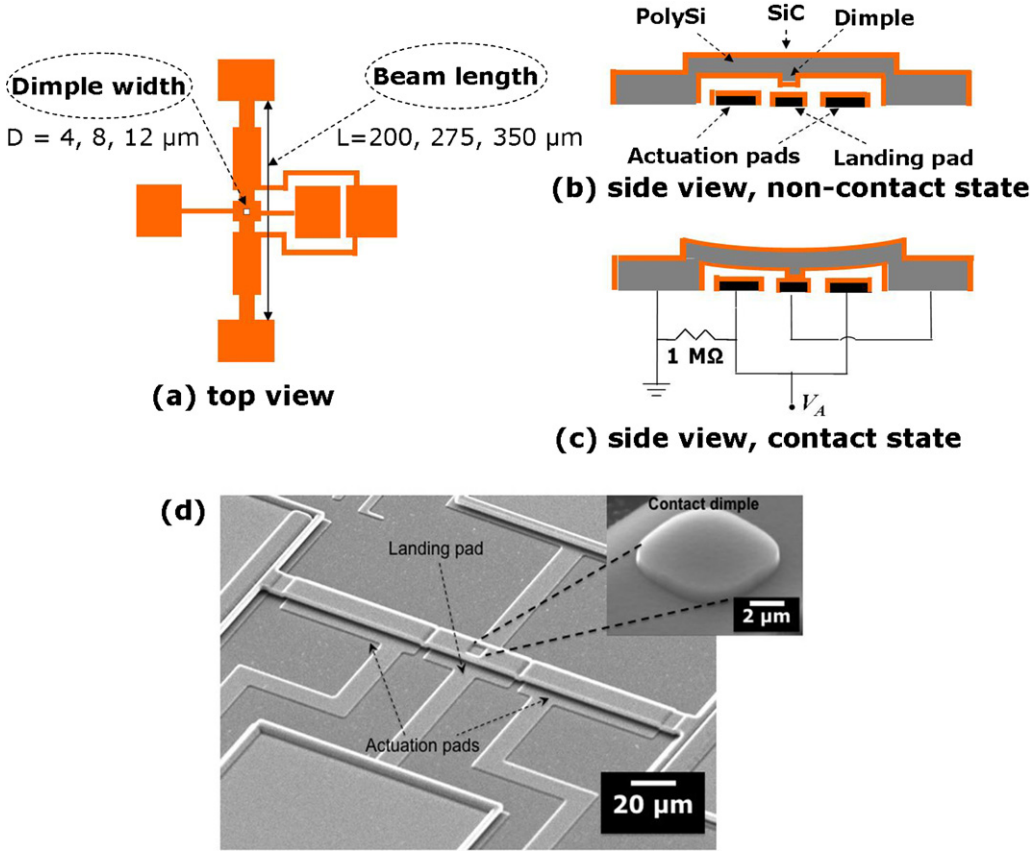

Fig. 1. (a)–(c) Schematic representations of the electrostatically actuated double-clamped beam test structure. The same designs were also coated with a polycrystalline SiC film for comparison. (d) Representative SEM micrograph of a 275 μm long polysilicon DCB device (inset is an inverted dimple).

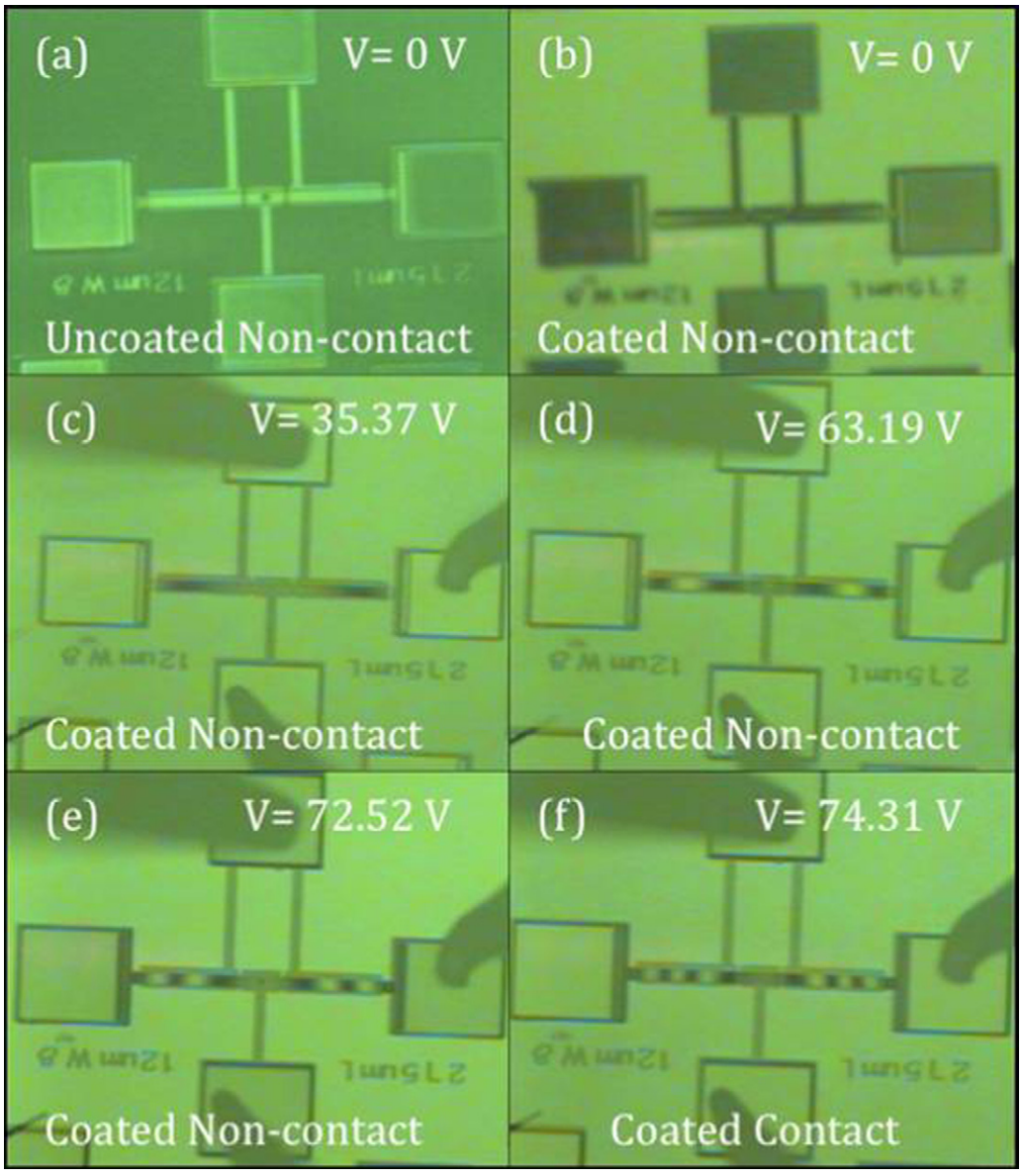

Fig. 2. (a) Interferometric image of as-fabricated polysilicon test structure. (b)–(f) Interferometric images of SiC-coated structure at various applied voltages as the beam was brought into contact with the landing pad electrostatically.

conditions for the DCB adhesion test structures. Fig. 2 shows the DCB device as fabricated (a) and after SiC coating (b) and at various applied voltages (c–f). The interferometric image of the beam before any applied bias (Fig. 2b) shows that residual strain upon SiC coating is minimal and has little to no effect in the calculation of cantilever spring constant. Fig. 3 summarizes the beam profile vs. applied bias deduced from interferometric images.

The adhesion force between the contacting surfaces is calculated as follows:

$$F_{adh} = k\Delta z - \left(\frac{1}{2}\right) w\varepsilon_o V_{pull-off}^2 2 \int_0^x \frac{dx}{g^2(x)} \quad (1)$$

where k represents the cantilever spring constant, Δz is the beam displacement during substrate contact, w is the actuation electrode width, ε_o is permittivity of air, $V_{pull\text{-}off}$ is the voltage at which the beam releases from contact, and g is the gap distance between the beam and landing pad at the actuation pad length, x. The first term represents the cantilever spring restoring force, and the second term is the opposing electrostatic force acting on a deformable capacitor.

2.3. Lifetime studies

To study the evolution of microscale contacts as a function of number of impact cycles, two separate as-fabricated polysilicon and SiC-coated devices with 12 μm × 12 μm contact dimples were each cycled at 60 kHz frequency through a sinusoidal voltage and an applied load of 5 V overdrive equivalent to 8 μN contact force, estimated using finite element simulation methods. The cyclic contact experiments were performed in an enclosed, airtight chamber at 25 °C and ~50% relative humidity. The humidity was maintained by purging the enclosed probe station (Signatone S-1160) continuously with dry air. A 50% humidity was chosen due to the fact that most Si-based microdevices operate under ambient atmospheric conditions. The devices were wirebonded using Al microwires and the actuation voltage (AC bias) was supplied from a home-built function generator. Longer devices were deliberately chosen for

lifetime studies on SiC-coated structures to bring the actuation voltage to <100 V in order to reduce charging effects from otherwise high electric fields. A 275 μm long polysilicon DCB and a 350 μm long SiC-coated DCB have comparable actuation voltages of ~25 V. Contact resistance vs. number of impacts was monitored through *I–V* measurements at set periods of cycling using a Keithley 2400 Sourcemeter instrument by the four-point method.

After cycling the devices to ~100 billion times, the suspended beams were removed to allow analyses of the impacted surfaces. The surface morphology and surface potential postmortem were characterized via atomic force microscopy (AFM) and Kelvin probe force microscopy (KPFM) through a Digital Instrument Nanoscope IIIa scanning probe microscope equipped with extender electronics module. Finally, chemical analysis of the impacted landing pads was accomplished through Auger electron spectroscopy (AES) and microscopy methods using a Physical Instruments, Inc. PHI 700 Scanning Auger Nanoprobe system. For comparison, a separate set of unactuated devices on the same die were removed and analyzed similarly.

3. Results and discussion

3.1. Adhesion force measurements

Fig. 4 summarizes the measured adhesion force for polycrystalline Si/Si and SiC/SiC contacts as a function of dimple area. As mentioned in the experimental section, the adhesion force for a given dimple size is calculated from the difference between the restoring and the electrostatic forces at pull-off. The former requires accurate determination of the spring constant from the actual beam profile while the latter involves measurement of the distributed gap between the beam and the actuation pads just prior to the beam separating from contact with the landing pad. The results demonstrate that polycrystalline SiC/SiC contacts exhibit lower adhesion compared to polycrystalline Si/Si despite the lower roughness of the SiC surfaces (10.2 nm vs. 15.1 nm for polysilicon). It is expected for rougher surfaces to exhibit lower adhesion forces due to reduced real contact area. The opposite trend observed here highlights the tribological benefit of intrinsically low surface energy and high hardness of SiC. The overall results also suggest that the adhesion force between rough, rigid surfaces scales weakly with the apparent contact area. The expected linear scaling with apparent area is still not seen in smoother SiC surfaces which highlights

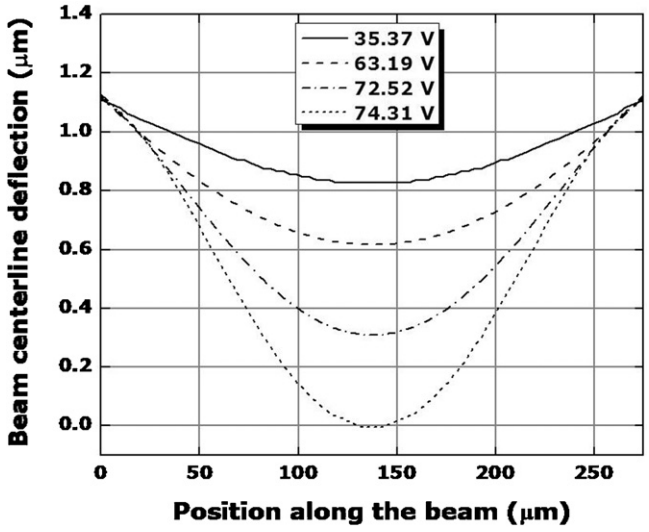

Fig. 3. Beam deflection profile deduced from interferometric image for 275-μm SiC-coated device at various applied voltages.

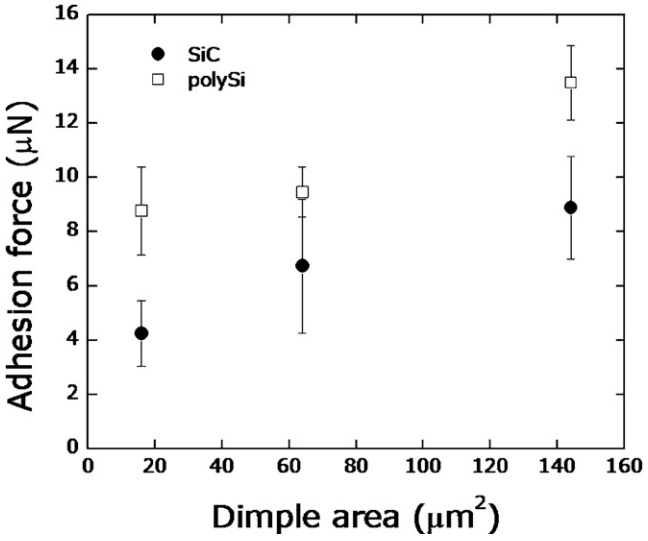

Fig. 4. Plot of adhesion force as a function of dimple area. Polycrystalline SiC/SiC-coated contacts exhibit lower adhesion compared to polycrystalline Si/Si.

that real contacts in rough surfaces involve only a few asperities [2,28].

It must be noted that the magnitude of adhesion force for a given dimple size in this study is generally lower compared to the previous polyMUMPs fabrication run [27]. The discrepancy is ascribed to roughness variation, i.e. devices in the current generation are 1.5 times rougher than the previous fabrication run reported in Ref. [27]. These findings underscore the importance of thorough characterization of interacting surfaces as different fabrication runs could yield large variations in surface morphology which is directly related to the measured adhesion force once surfaces are brought into contact.

3.2. Lifetime studies

A figure of merit for predicting MEMS reliability is based on reliable electrical and tribological performance of devices in excess

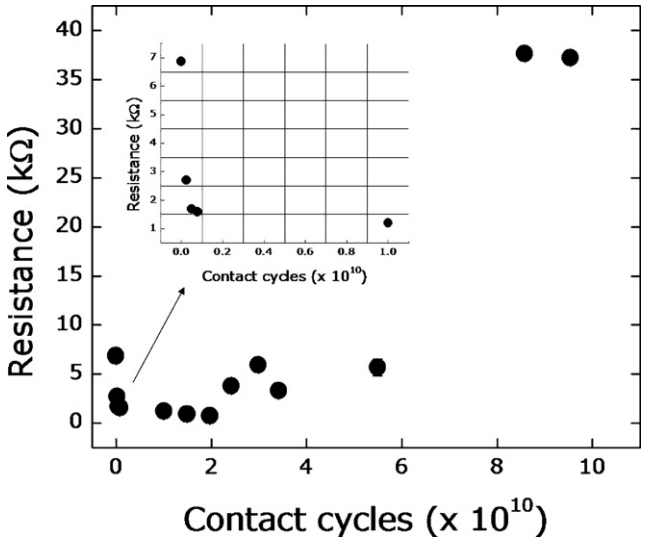

Fig. 5. Contact resistance of polySi/polySi device as a function of number of impacts. Initially during the first 10 billion cycles, contact resistance decreases as a function of number of impacts, then increases abruptly after ~50 billion cycles, ascribed to the generation of a single piece of wear debris (fractured grain) which breaks loose, leading to a high-resistance point contact.

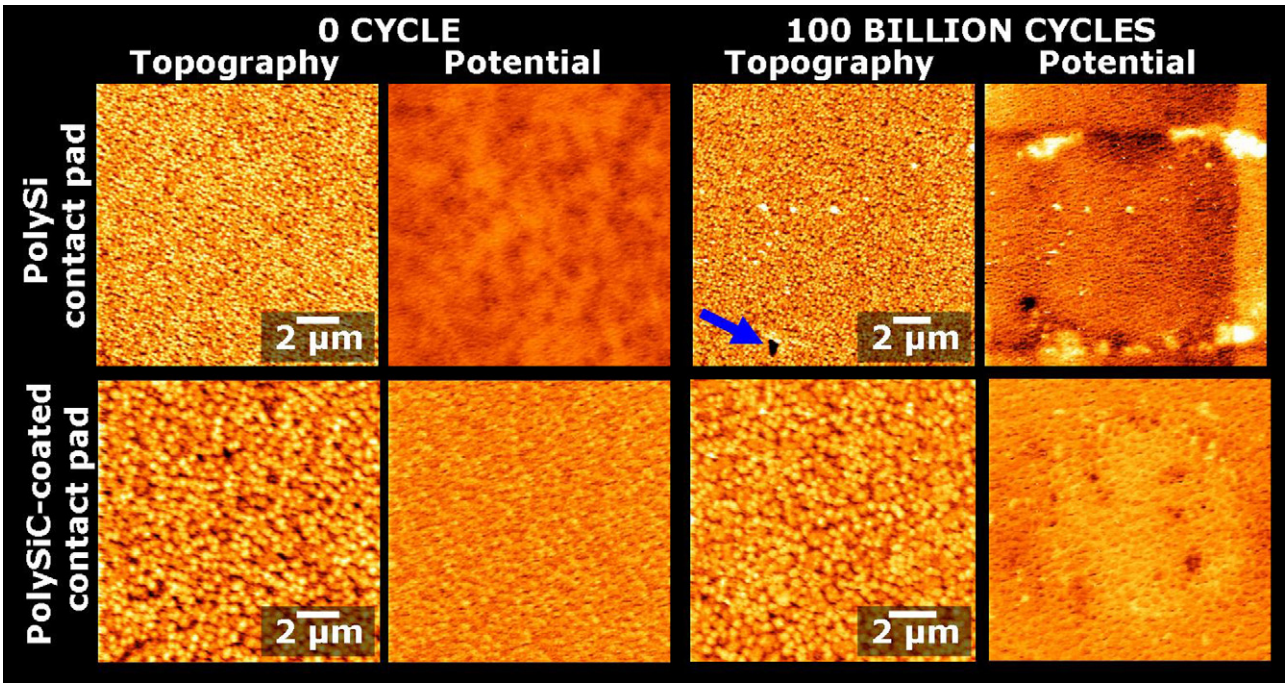

Fig. 6. AFM and KPFM images of the landing pads (top panel: polysilicon; lower panel: SiC) prior to any impact and after 100 billion cycles. An arrow is drawn to highlight a crater formed on the impacted polysilicon surface. Roughness (rms) of landing pads before any impacts: 15.1 nm (polysilicon) and 10.2 nm (polySiC). The z-scales are 500 nm and 200 mV, respectively.

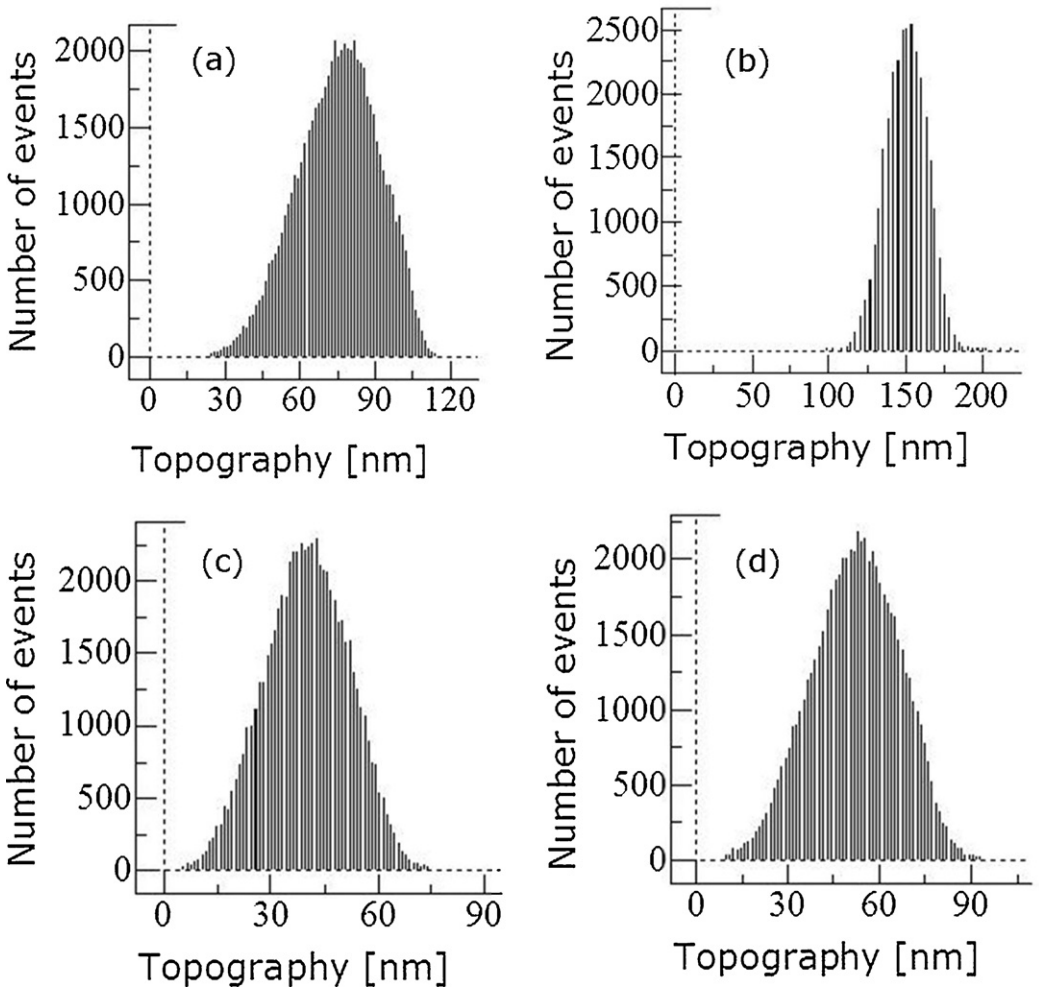

Fig. 7. Roughness histograms of the landing pads: (a) as-fabricated polysilicon, (b) polysilicon after 100 billion contacts, (c) SiC-coated polysilicon prior to any impact, and (d) SiC-coated polysilicon after 100 billion cycles.

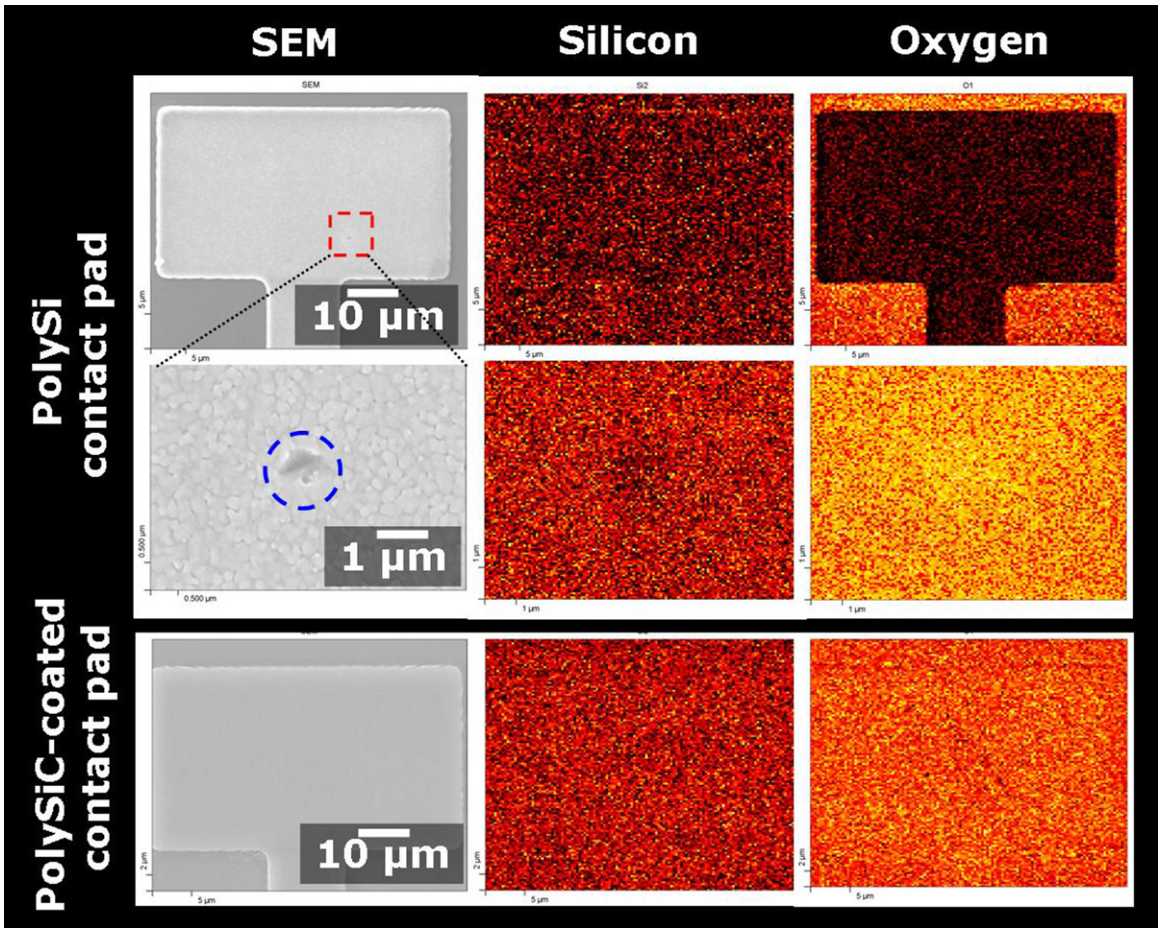

Fig. 8. Scanning Auger electron analysis on the impacted landing pads. Left panels: secondary electron image of the contact pads; middle and right panels: relative silicon and oxygen concentration maps indicating higher degree of oxidation on the worn surface of polysilicon (as indicated by more intense, bright Auger signal) after 100 billion contact cycles. A circle is drawn to highlight the worn area on polysilicon contact pad.

of tens of billions of contact cycles [29–31,33]. To assess long-term reliablity, lifetime studies on SiC-coated structures and on as-fabricated polysilicon with native oxide were performed by following the microscale changes in physical, chemical, and electrical properties [35,36] of both interfaces upon cyclic loading. The inherent low surface energy of SiC afforded measurements performed using devices with longer beams without suffering from permanent adhesion.

The electrical properties of polysilicon surfaces were monitored via four-point *I–V* measurements and the measured contact resistance vs. number of impact cycles is summarized in Fig. 5. An initial decrease in resistance is observed, attributed to asperity flattening, and after ~50 billion cycles, the resistance increases abruptly, reaching to about 40 kΩ after 90 billion cycles. A decrease in contact resistance at an early stage of cyclic experiments is in agreement with the behavior previously observed on polySi/polySi contact studies, albeit performed via a single-clamped, 2-axis MEMS deflecting cantilever (2-AMDC) device with 3 μm-diameter dimple size [32]. This phenomenon is ascribed to flattening of asperity summits characteristic of rough and rigid interacting surfaces. Asperity flattening typically is observed during the first few tens of million cycles for polySi surfaces [32] with roughness of ~10 nm and even at much lower applied loads (tens of nN). The contact resistance for undoped SiC, on the other hand, caused the current to fall outside the ammeter detection limit (<10 pA). This has been verified at least three times throughout the duration of over 100 billion contact cycles.

After 100 billion cycles, the beams were removed to allow analyses of both impacted surfaces. Fig. 6 displays the AFM/KPFM images of the landing pad before any impact and after 100 billion cycles. Results indicate little change to the SiC surface morphology and suggest wear resistance under relatively high impact forces. In contrast, impacted polysilicon exhibited wear debris and crater-like surface features indicative of grain fracture from cyclic loading, consistent with previous studies using 2AM-DC test structure [32]. This crater-like surface reduces the effective contact area and thus increases the contact resistance measured. Surface potential images also indicate that the impacted region is chemically different after 100 billion contacts.

Fig. 7 compares the roughness histograms of as-fabricated landing pads and after 100 billion contact cycles. A comprehensive amplitude-based surface roughness analysis suggests that polysilicon became significantly rougher [by comparing the average height of grains between the un-impacted (a) =~72 nm and postmortem (b) =150 nm]. The average roughness of SiC-coated landing pad, on the other hand, remain virtually unchanged before (c) and after 100 billion cycles (d).

The ratio of oxygen to silicon concentration as determined from AES analysis of the landing pad is higher in the worn areas of polysilicon (Table 1), in comparison with its unimpacted counterpart. This is consistent with the elevated surface potential observed from KPFM analysis of the impacted polysilicon surface. Higher degree of oxidation is ascribed to the removal of the native oxide layer from repetitive impacts between the asperity summits that are in direct contact. As fresh silicon surface is exposed to

Table 1
Summary of ratios atomic concentrations of oxygen to silicon ([O]/[Si]) on the interacting surfaces as determined through AES analysis.

	Polysilicon		SiC	
	Landing pad	Dimple	Landing pad	Dimple
As-fabricated	0.48	0.47	0.12	0.61
After 100 billion cycles	8.6	1.6	0.14	0.72

atmosphere, further oxidation occurs and is accelerated in worn, high surface area regions. In contrast, much lower degree of oxidation was observed in the impacted SiC landing pad.

Fig. 8 displays spatially resolved silicon and oxygen concentrations on the contact pads obtained from scanning AES. The results suggest that the slight contrast in surface potential observed in impacted SiC is not directly related to oxidation but rather may be due to surface fatigue, which affects the work function [34]. The structural changes that may exist beneath the SiC surface due to subsurface fatigue may be responsible for the observed changes in surface potential even in the absence of wear. In contrast, AES analysis reveals that oxygen concentration is higher in the worn, impacted surfaces of polysilicon (Fig. 8), which explains the elevated surface potential in the contact zone.

4. Conclusions

This work illustrates device-level measurements of adhesion forces and cyclic impact studies directly comparing polysilicon and polySiC interfaces. The dependence of stiction on apparent area of contact (as defined by microfabricated dimples) has been quantified for both material systems. It was observed that polycrystalline SiC exhibit adhesion forces less than half those on polysilicon. This work further documents the evolution of morphological, electrical, and chemical properties of polysilicon and polySiC surfaces undergoing cyclic contacts for over 100 billion times. The above approach highlights the beneficial effect of a thin silicon carbide coating on polysilicon by enhancing contact reliability. More specifically, it was seen that SiC coating suppresses the rate of adhesive wear and grain fracture: little change to the SiC surface morphology and suggest wear resistance under relatively high impact forces for over 100 billion cycles; in contrast to polysilicon which exhibited wear debris and crater-like surface features indicative of grain fracture from cyclic loading. The devices remained resilient to failure from stiction due to low surface energy in the presence of SiC coating, and to accelerated mechanical stress due to hardened contacting surfaces. More compliant (longer) devices have been successfully actuated owing to low surface energy nature of SiC coating. This work further demonstrates that surface modification of silicon-based microdevices through thin SiC coating after microstructure release is an effective approach to suppress stiction and wear-related failure mechanisms while avoiding constraints on the front-end fabrication steps.

Acknowledgments

This work was supported in part by the Defense Advanced Research Projects Agency (DARPA) N/MEMS S&T Fundamentals program under grant no. N66001-10-1-4004 issued by the Space and Naval Warfare Systems Center Pacific (SPAWAR). Support from Robert Bosch GmbH and STMicroelectronics is also gratefully acknowledged. The authors also thank Nathan Klejwa for assistance in the AES analysis, Prof. Roger T. Howe (Stanford University) for helpful discussion, Dr. Fang Liu for assistance with the device design and packaging, and Yongkwan Kim for assistance with the AFM/SEM analysis.

References

[1] R. Maboudian, R.T. Howe, Critical Review, Adhesion in surface micromechanical structures, Journal of Vacuum Science and Technology B 15 (1997) 1–20.
[2] R. Maboudian, C. Carraro, Surface chemistry and tribology of MEMS, Annual Review of Physical Chemistry 55 (2004) 35–54.
[3] W.R. Ashurst, M.P. de Boer, C. Carraro, R. Maboudian, An investigation of sidewall adhesion in MEMS, Applied Surface Science 212–213 (2003) 735–741.
[4] K. Komvopoulos, Adhesion and friction forces in microelectromechanical systems: mechanisms, measurement, surface modification techniques, and adhesion theory, Journal of Adhesion Science and Technology 17 (2003) 477–517.
[5] N.R. Tas, C. Gui, M. Elwenspoek, Static friction in elastic adhesion contacts in MEMS, Journal of Adhesion Science and Technology 17 (2003) 547–561.
[6] J.H. Lee, H.H. Chung, S.Y. Kang, J.T. Baek, H.J. Yoo, Fabrication of surface micromachined polysilicon actuators using dry release process of HF gas phase etching, in: IEEE Trans. Electron Devices, San Francisco, CA, USA, December 8–11, 1996, pp. 761–764.
[7] F. Kozlowski, N. Lindmair, Th. Scheiter, C. Hierold, W. Lang, A novel method to avoid sticking of surface-micromachined structures, Sensors and Actuators A 54 (1996) 659–662.
[8] J. Anguita, F. Briones, HF/H_2O vapor etching of SiO_2 sacrificial layer for large-area surface-micromachined membranes, Sensors and Actuators A 64 (1998) 247–251.
[9] M. Offenberg, B. Elsner, F. Larmer, Vapor HF etching for sacrificial oxide removal in surface micromachining, Proc, in: Proc. Electrochemical Society Meeting, vol. 94, October 2, 1994, 1994, pp. 1056–1057.
[10] W.R. Ashurst, C. Carraro, R. Maboudian, W. Frey, Wafer level anti-stiction coatings with superior thermal stability, Sensors and Actuators A 104 (2003) 213–221.
[11] T.M. Mayer, M.P. de Boer, N.D. Shinn, P.J. Clews, T.A. Michalske, Chemical vapor deposition of fluoroalkylsilane monolayer films for adhesion control in microelectromechanical systems, Journal of Vacuum Science and Technology B 18 (2000) 2433–2440.
[12] G.T. Mulhern, D.S. Soane, R.T. Howe, Proc. 7th Int. Conf. On Solid-State Sensors and Actuators, Transducers '93, Yokohama, Japan, 1993, pp. 296–300.
[13] M.R. Houston, R.T. Howe, R. Maboudian, Effect of hydrogen termination on the work of adhesion between rough polycrystalline silicon surfaces, Journal of Applied Physics 81 (1997) 3474–3483.
[14] R.L. Alley, P. Mai, K. Komvopolous, R.T. Howe, Surface roughness modification of interfacial contacts in polysilicon microstructures, in: Proc. 7th Int. Conf. Solid-State Sensors and Actuators, Transducers '93, Yokohama, Japan, 1993, pp. 288–291.
[15] Y. Yee, K. Chun, J.D. Lee, Polysilicon surface modification technique to reduce sticking of microstructures, in: Proc. Int. Conf. Solid-State Sensors and Actuators, Transducers '95, Stockholm, Sweden, 1995, pp. 206–209.
[16] I. Laboriante, M. Fisch, A. Payamipour, F. Liu, C. Carraro, R. Maboudian, Morphological, electrical, and chemical changes in cyclically contacting polycrystalline silicon surfaces coated with perfluoroalkylsilane self-assembled monolayer, Tribology Letters 44 (2011) 13–17.
[17] W.R. Ashurst, C. Yau, C. Carraro, R. Maboudian, M.T. Dugger, Dichlorodimethylsilane as an anti-stiction monolayer for MEMS: a comparison to the octadecyltrichlosilane self-assembled monolayer, Journal of Microelectronic Systems 10 (2001) 41–49.
[18] J. Fréchette, R. Maboudian, C. Carraro, Effect of temperature on in-use stiction of cantilever beams coated with perfluorinated alkysiloxane monolayers, Journal of Microelectronic Systems 15 (2006) 737–744.
[19] A. Ulman, An Introduction to Ultrathin Organic Films: from Langmuir–Blodgett to Self-Assembly, Academic Press, London, 1991.
[20] R. Maboudian, W.R. Ashurst, C. Carraro, Self-assembled, monolayers as anti-stiction coating for MEMS: characteristics and recent progress, Sensors and Actuators A 82 (2000) 219–223.
[21] R. Maboudian, W.R. Ashurst, C. Carraro, Tribological challenges in MEMS, Tribology Letters 12 (2002) 95–100.
[22] T.-H. Lee, S. Bhunia, M. Mehregany, Electromechanical computing at 500 degrees C with silicon carbide, Science 329 (2010) 1316–1318.
[23] N. Rajan, M. Mehregany, C.A. Zorman, S. Stefanescu, T.P. Kicher, Fabrication and testing of micromachined silicon carbide and nickel fuel atomizers for gas turbine engines, Journal of Microelectronic Systems 8 (1999) 251–257.
[24] P. Godignon, SiC materials and technologies for sensors development, Materials Science Forum 483 (2004) 1009–1014.
[25] M. Willander, M. Friesel, Q.U. Wahab, B. Straumal, Silicon carbide and diamond for high temperature device applications, Journal of Materials Science: Materials in Electronics 17 (2006) 1–25.
[26] D. Gao, C. Carraro, R.T. Howe, R. Maboudian, Polycrystalline silicon carbide as a substrate material for reducing adhesion in MEMS, Tribology Letters 21 (2006) 226–232.
[27] G.H. Li, I. Laboriante, F. Liu, M. Shavezipur, B. Bush, C. Carraro, R. Maboudian, Measurement of adhesion forces between polycrystalline silicon surfaces via a MEMS double-clamped beam test structure, Journal of Micromechanics and Microengineering 20 (2010) 095015.
[28] I. Laboriante, B. Bush, D. Lee, F. Liu, T.-J. King-Liu, C. Carraro, R. Maboudian, Interfacial adhesion between rough surfaces of polycrystalline silicon and its implications for M/NEMS technology, Journal of Adhesion Science and Technology 24 (2010) 2545–2556.

[29] J.C.M. Hwang, Reliability of electrostatically actuated RF MEMS switches, in: Proc. IEEE Int. Workshop on Radio-Frequency Integration Technology: Enabling Technologies for Emerging Wireless Systems, Singapore, 2007, pp. 168–171.
[30] J.J. Yao, RF MEMS from a device perspective, Journal of Micromechanics and Microengineering 10 (2000) R9–R38.
[31] E.A. Sovero, R. Mihailovich, D.S. Deakin, J.A. Higgins, J.J. Yao, J.F. DeNatale, J.H. Hong, Monolithic GaAs PHEMT MMICs integrated with high performance MEMS microrelays, in: Proc. SBMO/IEEE, MTT-S International Microwave and Optoelectronics Conference, Rio de Janeiro, Brazil, 1999, pp. 257–260.
[32] F. Liu, I. Laboriante, B. Bush, C.S. Roper, C. Carraro, R. Maboudian, In situ studies of interfacial contact evolution via a 2-axis deflecting cantilever microinstrument, Applied Physics Letters 95 (2009) 131902.
[33] I. Laboriante, N. Klejwa, A. Suwandi, C. Carraro, R.T. Howe, R. Maboudian, Suppression of wear in cyclically loaded polycrystalline silicon MEMS via a thin silicon carbide coating, in: Proc. 16th IEEE Int. Conference on Solid-State Sensors, Actuators, and Microsystems (Transducers 2011), Beijing, China, 2011, pp. 2319–2322.
[34] B. Bhushan, A.V. Goldade, Kelvin probe microscopy measurements of surface potential change under wear at low loads, Wear 244 (2000) 104–117.
[35] A. Lumbantobing, L. Kogut, K. Komvopoulos, Electrical contact resistance as a diagnostic tool for MEMS contact interfaces, Journal of Microelectronic Systems 13 (2004) 977–987.
[36] W.M. van Spengen, MEMS reliability from a failure mechanisms perspective, Microelectronics and Reliability 43 (2003) 1049–1060.

Biographies

Ian Laboriante received his bachelor's degree in Chemistry from University of the Philippines in Diliman, and his Ph.D. also in Chemistry from the University of Houston. Dr. Laboriante pursued postdoctoral research in the laboratory of Prof. Maboudian at the University of California, Berkeley to investigate the tribology and surface science of M/NEMS materials and devices. He is currently affiliated with Micron Technology, Inc. in Boise, Idaho.

Anton Suwandi obtained his B.S. in Chemical Engineering from the University of California at Berkeley. His research interests include thin film science and technology and microsystems reliability.

Carlo Carraro is a researcher and a lecturer in the Department of Chemical and Biomolecular Engineering at the University of California, Berkeley. He received his bachelor's degree from the University of Padua, Padua, Italy, and his Ph.D. degree from California Institute of Technology in Pasadena, California. Dr. Carraro's research interests are in the physics and chemistry of surfaces and synthesis of novel thin-film materials and processes. He has coauthored over 140 papers in scholarly journals.

Roya Maboudian is a professor in the Department of Chemical and Biomolecular Engineering at the University of California, Berkeley. She received her Ph.D. degree from California Institute of Technology in Pasadena. Prof. Maboudian's research interest is in the surface and materials science and engineering of micro/nanosystems. The main research activities in her group currently include investigation of the tribological issues in M/NEMS and surface interactions in microfluidic environments; silicon carbide-based sensors for harsh environment applications; metallization of micro- and nano-devices; nanowire and graphene based sensors and energy technologies; and biologically inspired materials design. Prof. Maboudian is the recipient of several awards, including the Presidential Early Career Award for Scientists and Engineers, NSF Young Investigator award, and the Beckman Young Investigator award.